The end of the Dark Ages in MOND

Sławomir Stachniewicz, Marek Kutschera 2004

DESY Theory Workshop 2004

1. What is MOND?

MOdified Newtonian Dynamics (MOND) was suggested by Milgrom in 1983 and it has to replace non-baryonic dark matter. It assumes there is some parameter a_0 that

$$a = a_{Newton} \qquad a \gg a_0$$

$$\frac{a^2}{a_0} = a_{Newton} \qquad a \ll a_0$$

(modified dynamics) or

$$g = g_{Newton} \qquad g \gg a_0$$

$$g = \sqrt{g_{Newton} a_0} \qquad g \ll a_0$$

(modified gravity).

Sanders, Verheijen 1998 found the best-fit a_0

$$a_0 = (1.2 \pm 0.8) \times 10^{-8} \mathrm{cm/s^2}.$$

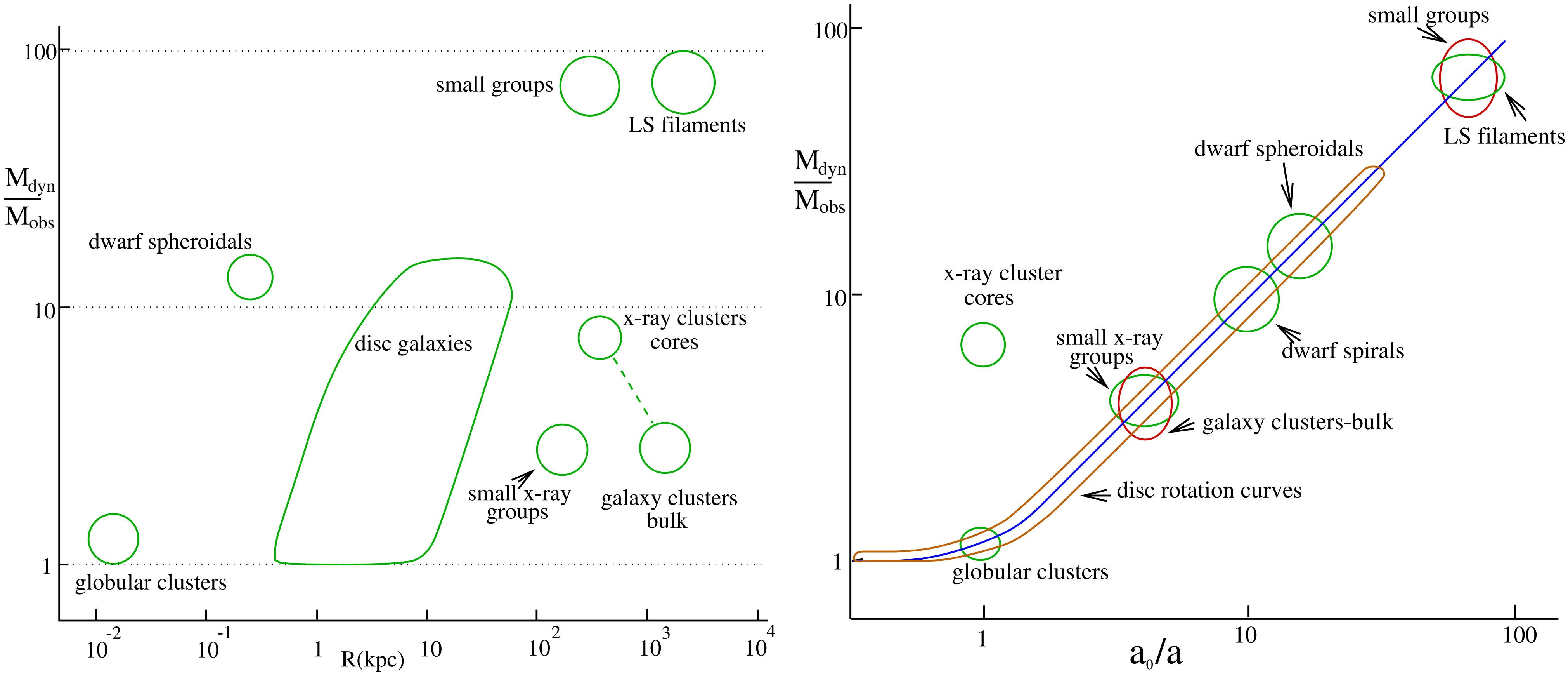

Milgrom, astro-ph/9810302

Problems:

$\Rightarrow$ inconsistent with General Relativity

$\Rightarrow$ nonlinear

$\Rightarrow$ what is $\boldsymbol{a}_0$?

Sanders, 1998: for $\boldsymbol{z > 3}$ MOND area is lower than the event horizont so probably for large $\boldsymbol{z}$ it does not affect the scale factor so it is enough to take background Friedmann models.

2. What are the Dark Ages of the Universe?

The Dark Ages is the period between recombination of hydrogen and appearance of the first sources of light (Pop. III objects). During the Dark Ages ionization is almost zero but the first sources of light re-ionize matter. Observations: for low z the Universe is ionized almost completely, the first non-ionized areas appear only for $z \sim 6$.

If one wants to trace evolution of a collapsing cloud, it is necessary to perform numerical simulations, usually 3-D. We have developped a 1-D hydrodynamical Lagrangian code (spherically symmetric) which is suitable for the highest overdensity peaks.

In the Newtonian case dynamics is governed by the following equations:

$$\frac{dM}{dr} = 4\pi r^2 \varrho$$

$$\frac{dr}{dt} = v$$

$$\frac{dv}{dt} = -4\pi r^2 \frac{dp}{dM} - \frac{GM(r)}{r^2}$$

$$\frac{du}{dt} = \frac{p}{\varrho^2} \frac{d\varrho}{dt} + \frac{\Lambda}{\varrho}$$

EOS of a perfect gas:

$$p = (\gamma - 1)\varrho u$$

where $\gamma = 5/3$ (mainly monoatomic H and He, fraction of H_2 does not exceed 10^{-3}).

If we modify gravity, the equation for $\frac{dv}{dt}$ will look a bit different:

$$\frac{dv}{dt} = -4\pi r^2 \frac{dp}{dM} - g_H - a_0 f\left(\frac{GM(r)}{a_0 r^2} - \frac{g_H}{a_0}\right)$$

where

$$g_H = \frac{1}{2} H_0{}^2 \left[(z+1)^3 \Omega_B + 2\left((z+1)^4 \Omega_r - \Omega_\Lambda\right)\right] r$$

and $f(x)$ is a function that interpolates between pure Newtonian and pure MOND limits. We have chosen

$$f(x) = \sqrt{1 + \sqrt{1 + (2/x)^2}/2}.$$

Our gas consists of H, H^-, H^+, He, He^+, He^{++}, H_2, H_2^+ and e^- and their abundances vary with time due to various chemical reactions.

3. Algorithm and initial conditions.

In the simulations we have used the code described in Stachniewicz, Kutschera 2001, based on the codes described by Thoul and Weinberg (1995) and Haiman, Thoul and Loeb (1996). This is a standard, one-dimensional, second-order accurate Lagrangian finite-difference scheme. The only changes were modification of gravity and putting the dark matter fraction $\boldsymbol{\Omega}_{dm}$ equal to zero. However, it was necessary to make significant changes in initial conditions:

⇒ we started our simulations for the beginning of the matter-dominated era (for $\boldsymbol{h = 0.72}$, $\boldsymbol{T}_\gamma$=2.7277 K and $\boldsymbol{\Omega}_b = \boldsymbol{\Omega}_m = \mathbf{0.02}/\boldsymbol{h}^2$ $\boldsymbol{z}_{eq} = \mathbf{485}$)

$\Rightarrow$ initial abundances of all species were calculated by a separate program.

It is unclear what should be initial perturbations of baryonic matter as $\mathrm{CMBFAST}$ by Seljak and Zaldarriaga 1996 and a CMB anisotropy program by Sugiyama give different predictions but we have adopted a value from between, i.e. $\mathbf{10^{-9}}$.

Initial density profile was in the form of a single spherical Fourier mode used by Haiman, Thoul and Loeb:

$$\varrho_b(r) = \Omega_b \varrho_c (1 + \delta \frac{\sin kr}{kr})$$

where $\varrho_c = 3H^2/8\pi G$ is the critical density.

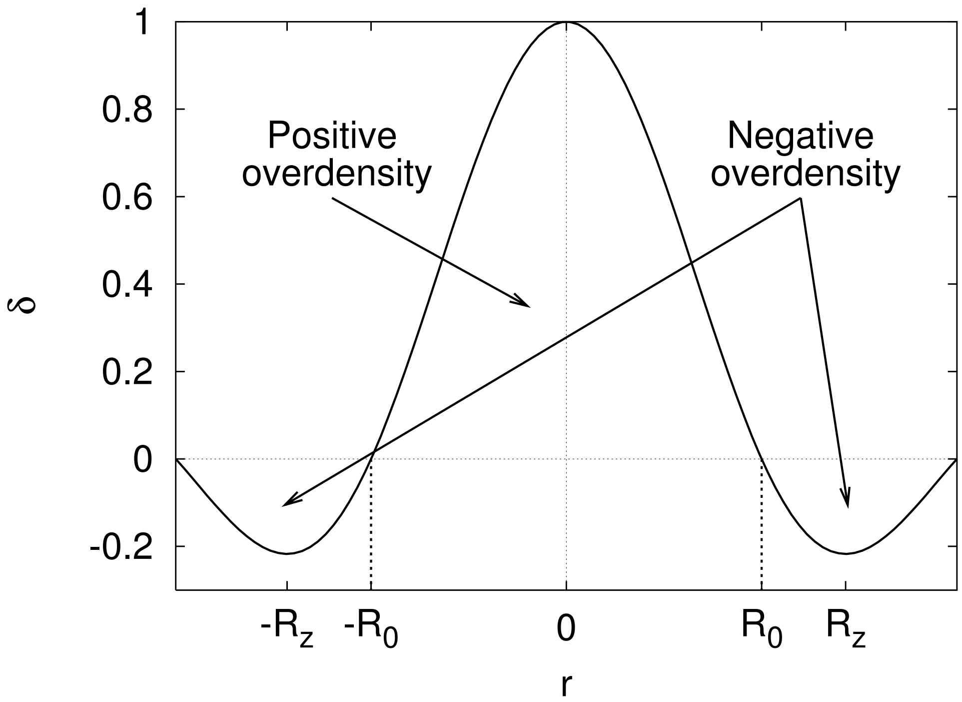

For this profile there exist two distinguished values of the radius, R_0 and R_z which correspond to the first zero and the first minimum of $\sin(kr)/kr$. Inside the sphere of radius $R_0 = \pi/k$ which contains mass M_0, local density contrast is positive. Local density contrast is negative for $R_z > r > R_0$, with average density contrast vanishing for the sphere of radius $\boldsymbol{R_z = 4.49341/k}$ with the mass $\boldsymbol{M_z}$. According to the gravitational instability theory in the expanding Universe, the shell of radius $\boldsymbol{R_z}$ will expand together with the Hubble flow not suffering any additional deceleration. This is why we regard this profile as very convenient in numerical simulations.

As the initial velocity we use the Hubble velocity:

$$\boldsymbol{v(r) = Hr}$$

4. Results.

We have performed 17 runs:

⇒ 8 for 'standard' $\boldsymbol{a}_0$ $(\mathbf{1.2} \times \mathbf{10}^{-8}\text{cm/s}^2)$, various $\boldsymbol{M}_0$ $(\mathbf{10}^3 \boldsymbol{M}_\odot$, $\mathbf{3} \times \mathbf{10}^3 \boldsymbol{M}_\odot$, $\mathbf{10}^4 \boldsymbol{M}_\odot$ and $\mathbf{3} \times \mathbf{10}^4 \boldsymbol{M}_\odot)$ and initial overdensities $(\mathbf{10}^{-9}$ and $\mathbf{10}^{-8})$

⇒ 3 for lower $\boldsymbol{a}_0$ $(\mathbf{1.2} \times \mathbf{10}^{-9}\text{cm/s}^2)$, $\mathbf{10}^{-9}$, $\boldsymbol{M}_0 = \mathbf{3} \times \mathbf{10}^3 \boldsymbol{M}_\odot$, $\mathbf{10}^4 \boldsymbol{M}_\odot$ and $\mathbf{3} \times \mathbf{10}^4 \boldsymbol{M}_\odot$

⇒ one for 'standard' $\boldsymbol{a}_0$ but without H_2 cooling

⇒ the other for 'standard' $\boldsymbol{a}_0$, we tried to estimate possible influence of fragmentation to structure formation in MOND.

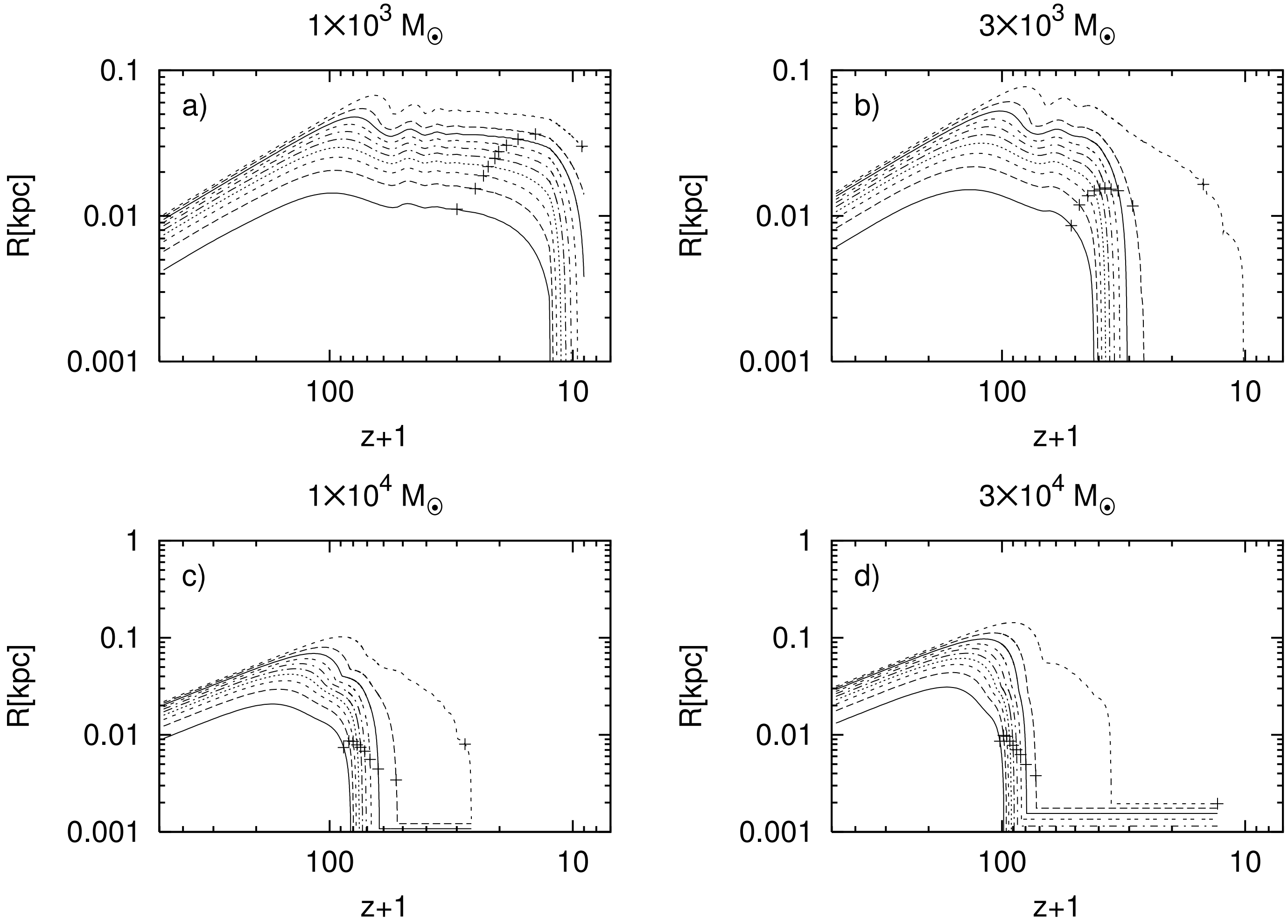

Shell trajectories for the 'standard' $\boldsymbol{a}_0$, $\mathbf{10^{-9}}$ overdensity.

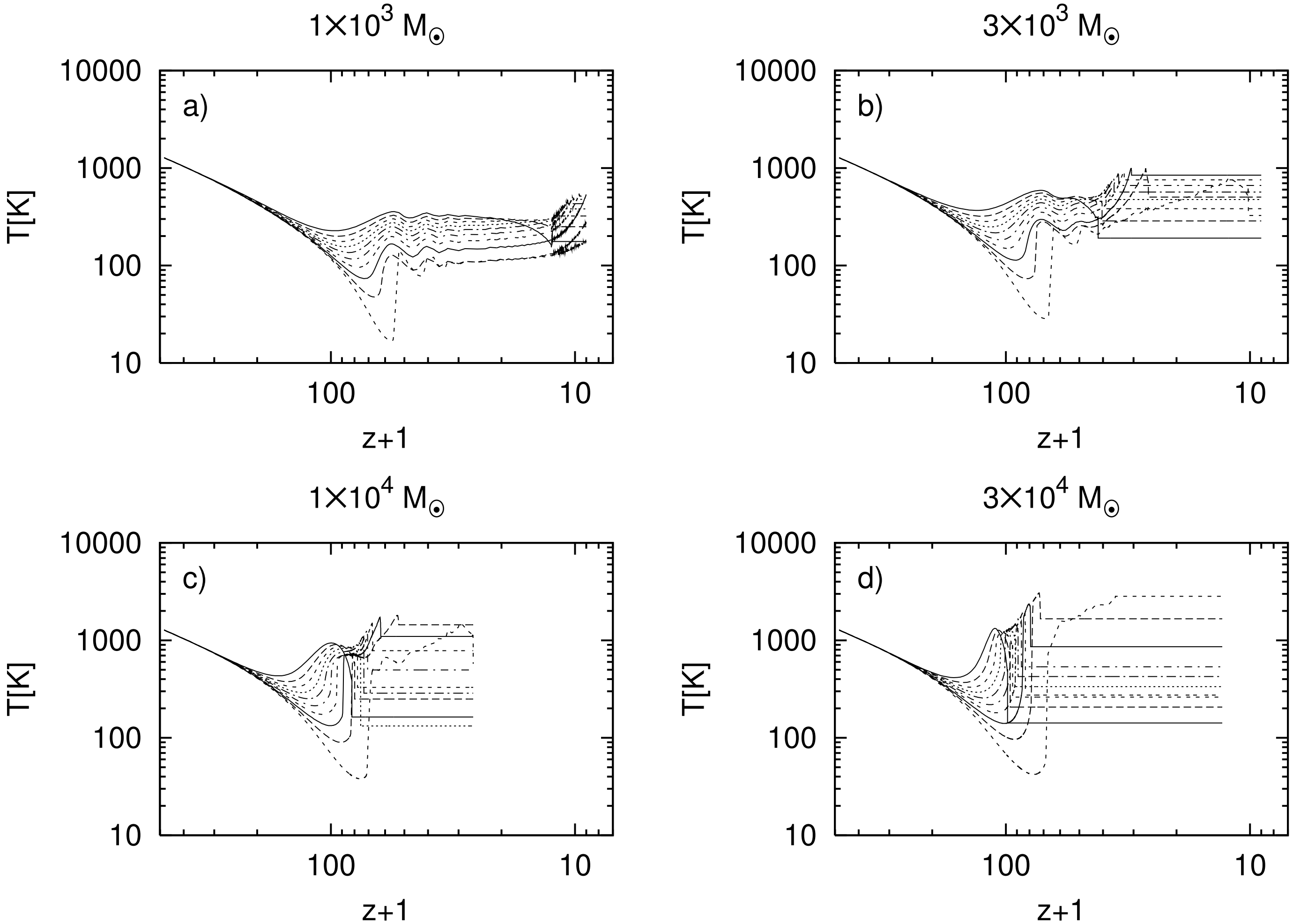

Shell temperaturs for the ‘standard’ $\boldsymbol{a}_0$, $\mathbf{10^{-9}}$ overdensity.

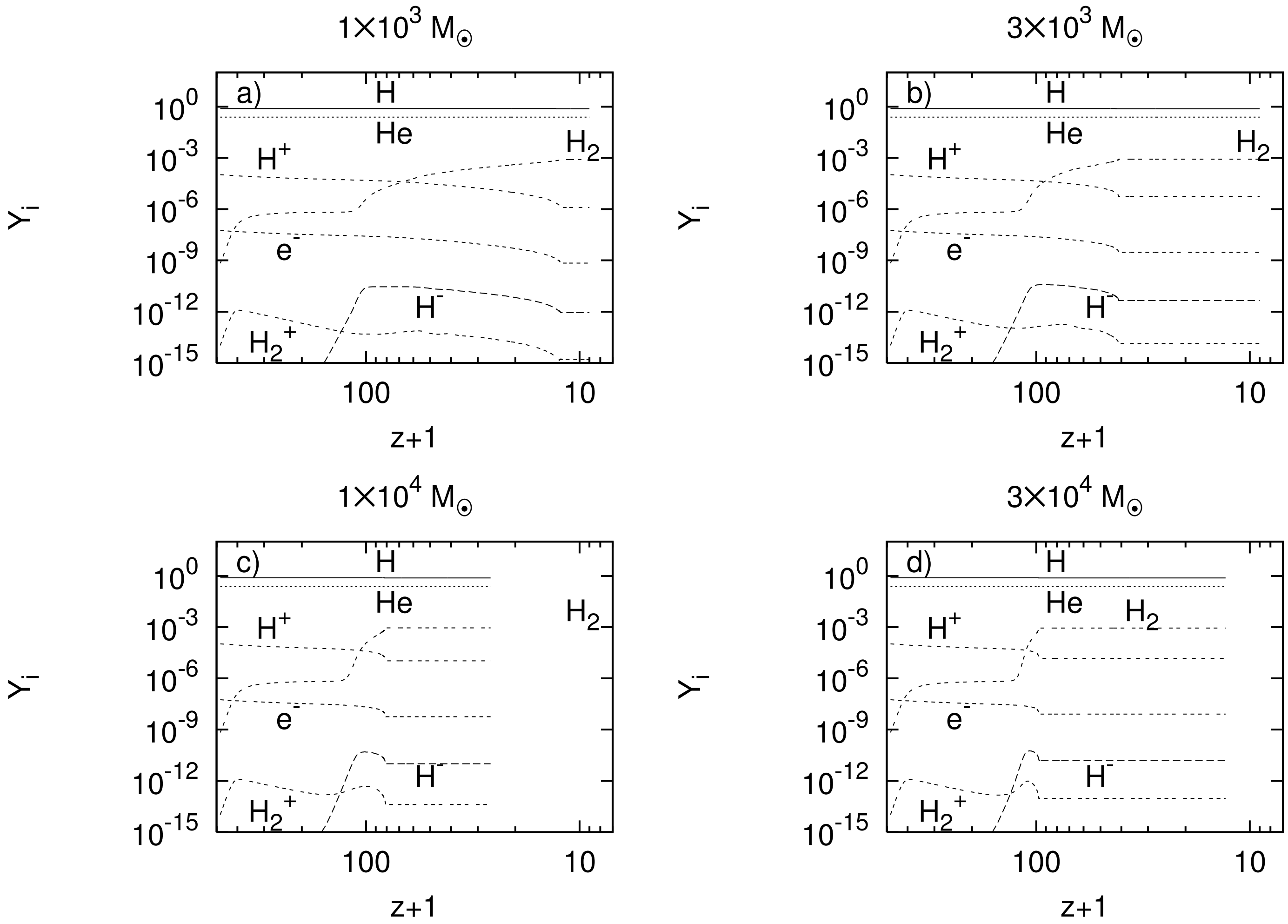

Chemical evolution for the 'standard' $\boldsymbol{a}_0$, $\mathbf{10}^{-9}$ overdensity.

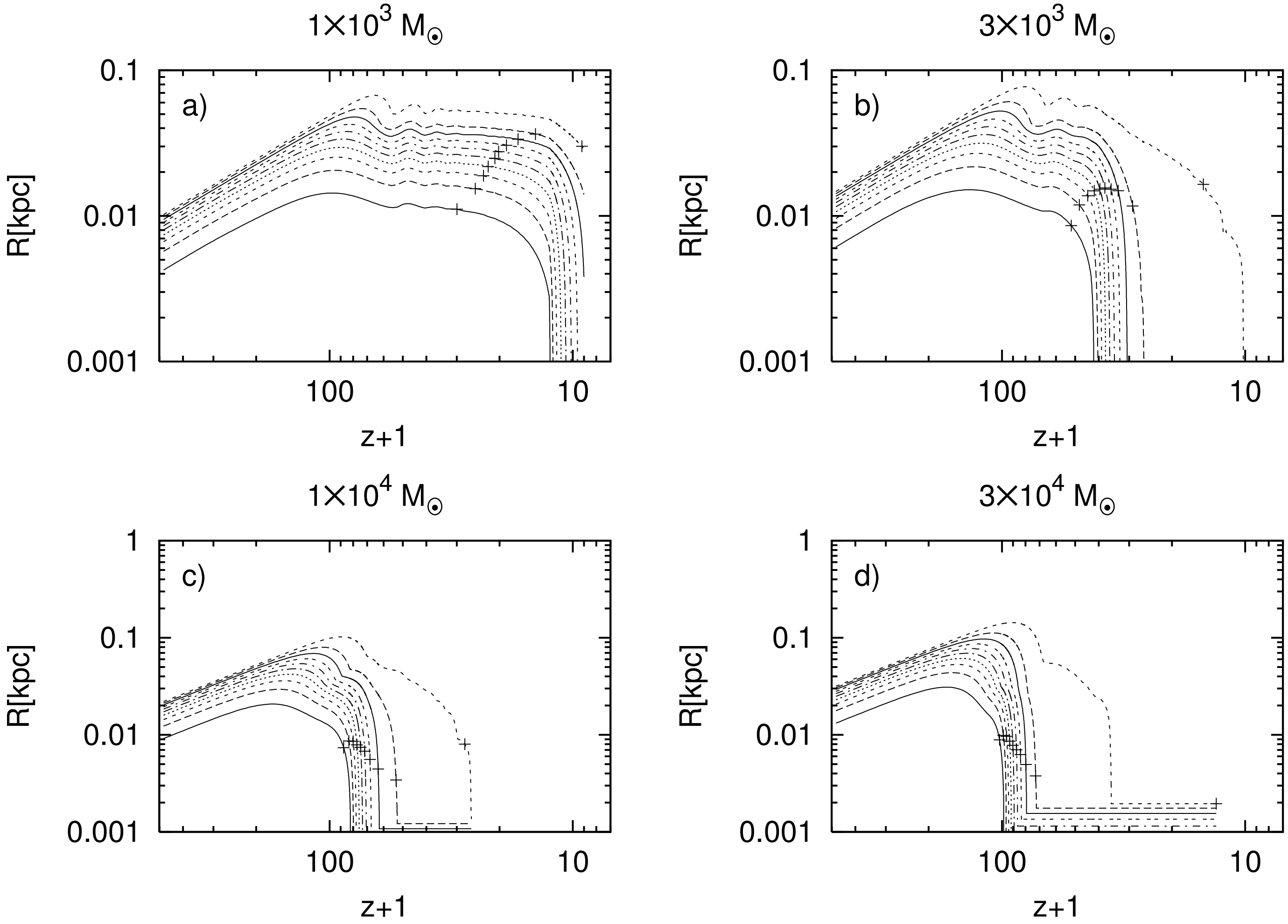

Shell trajectories for the 'standard' a_0, $\mathbf{10^{-8}}$ overdensity.

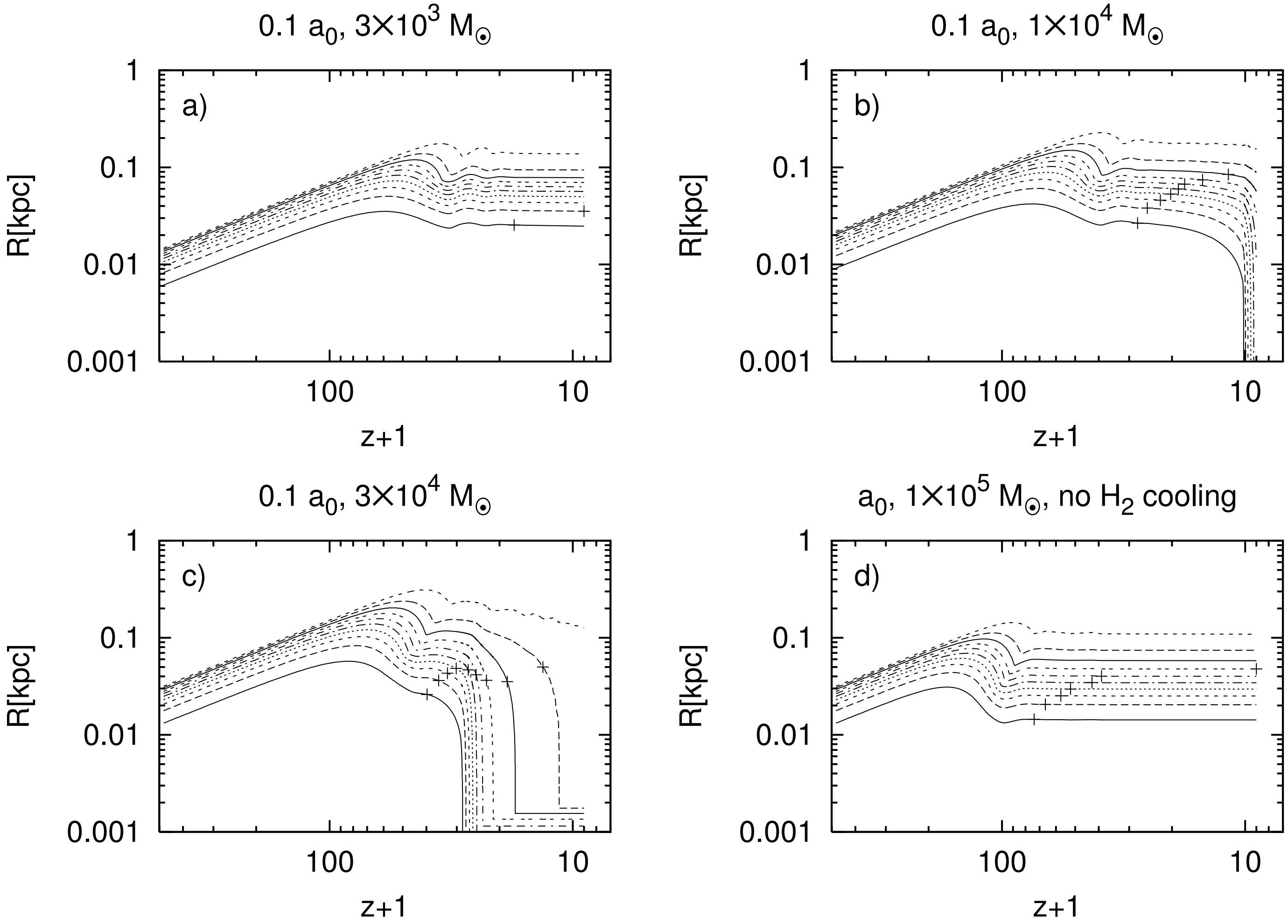

Shell trajectories for the 'low' $\boldsymbol{a}_0$, $\mathbf{10^{-9}}$ overdensity and ‘standard’ $\boldsymbol{a}_0$, $\mathbf{10^{-9}}$ overdensity, no H_2 cooling.

Most of these figures show trajectories of shells enclosing 7%, 17%, 27% ... 97% of the total mass. Conclusions:

⇒ the difference in behaviour between clouds with $\mathbf{10}^{-9}$ and $\mathbf{10}^{-8}$ overdensities is very tiny so results are much less sensitive to initial density contrast than in CDM

⇒ more massive clouds collapse faster

⇒ speed of collapse depends very strongly on $\boldsymbol{a}_0$

⇒ like in CDM models, H_2 cooling is necessary to collapse

⇒ like in CDM models, due to adiabatic cooling/heating shell temperatures behave opposite to the behaviour of shell radii, then H_2 cooling becomes important and the shells collapse; higher mass of the cloud means higher virial temperature and faster collapse

$\Rightarrow$ chemical evolution is quite typical but because the collapse is very violent, it makes chemical reactions much faster; however, final abundances of various species are not very different from predictions of the other models, e.g. final abundance of H_2 is in order of $\mathbf{10}^{-3}$.

The following figures were obtained when we tried to estimate possible influence of fragmentation to structure formation in MOND. To do so we have traced the evolution of a $\mathbf{10}^{6}\boldsymbol{M}_{\odot}$ cloud with $\mathbf{10}^{-9}$ overdensity until the most innermost shell had collapsed. Then we had taken the densities, temperatures, chemical composition etc. at that moment and re-scaled radii and velocities of all shells to obtain clouds of smaller masses and then traced their evolution.

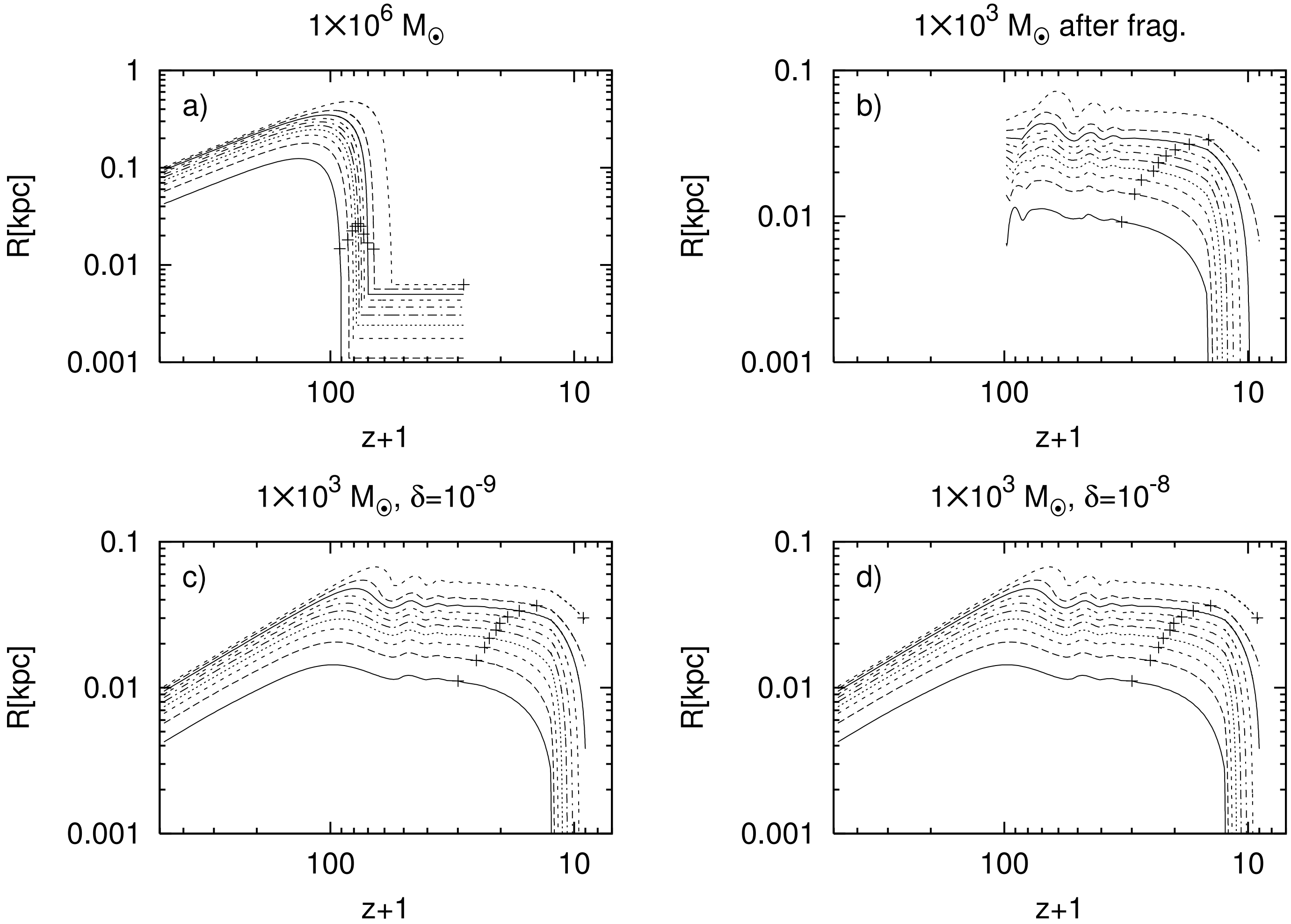

Shell trajectories for the 'standard' $\boldsymbol{a_0}$: $\mathbf{10^6} \boldsymbol{M_\odot}$ $\mathbf{10^{-9}}$, $\mathbf{10^3} \boldsymbol{M_\odot}$ after fragmentation, $\mathbf{10^3} \boldsymbol{M_\odot}$ $\mathbf{10^{-9}}$ and $\mathbf{10^3} \boldsymbol{M_\odot}$ $\mathbf{10^{-8}}$.

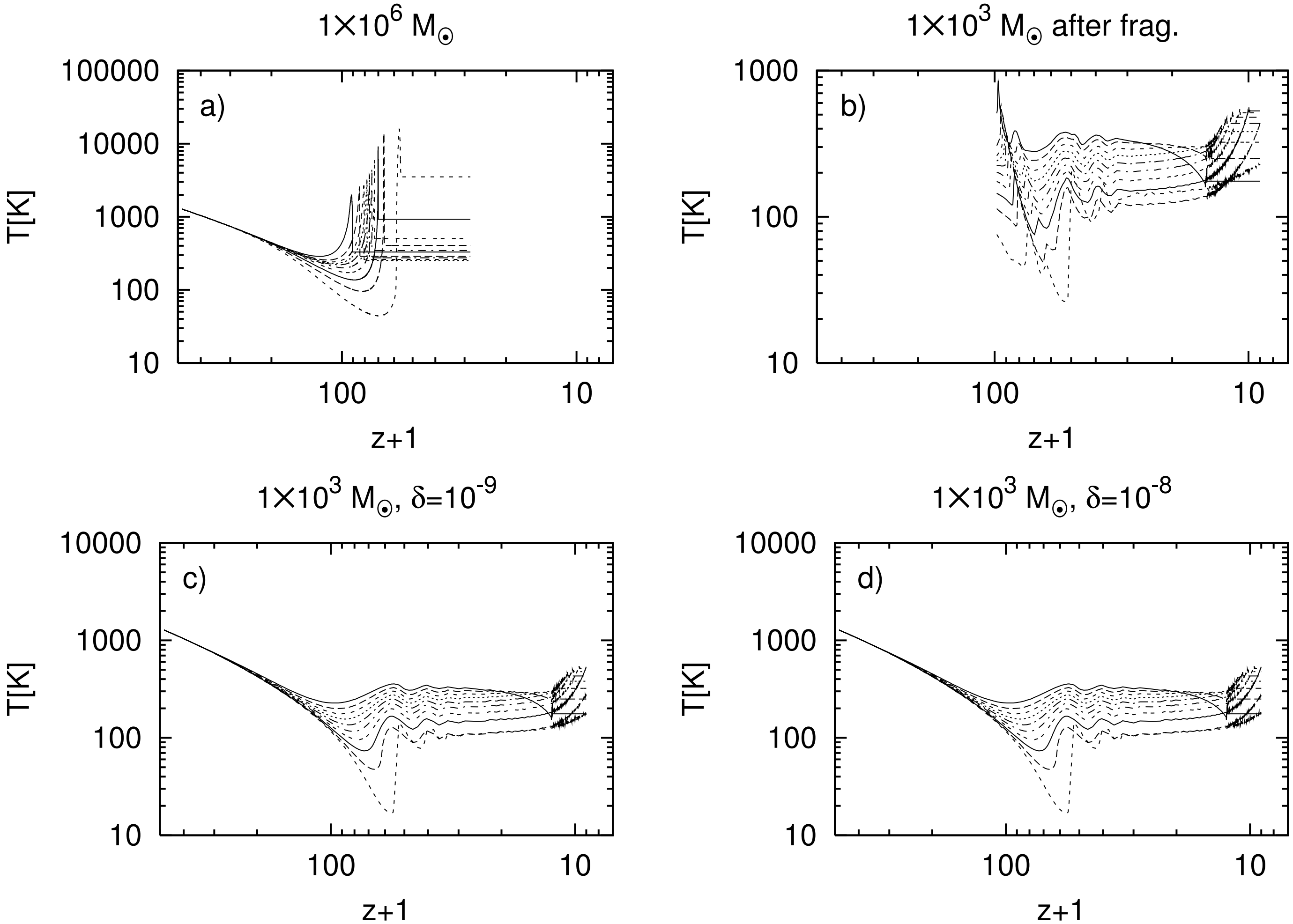

Shell temperatures for the ‘standard’ a_0: $10^6 M_\odot$ 10^{-9}, $10^3 M_\odot$ after fragmentation, $10^3 M_\odot$ 10^{-9} and $10^3 M_\odot$ 10^{-8}.

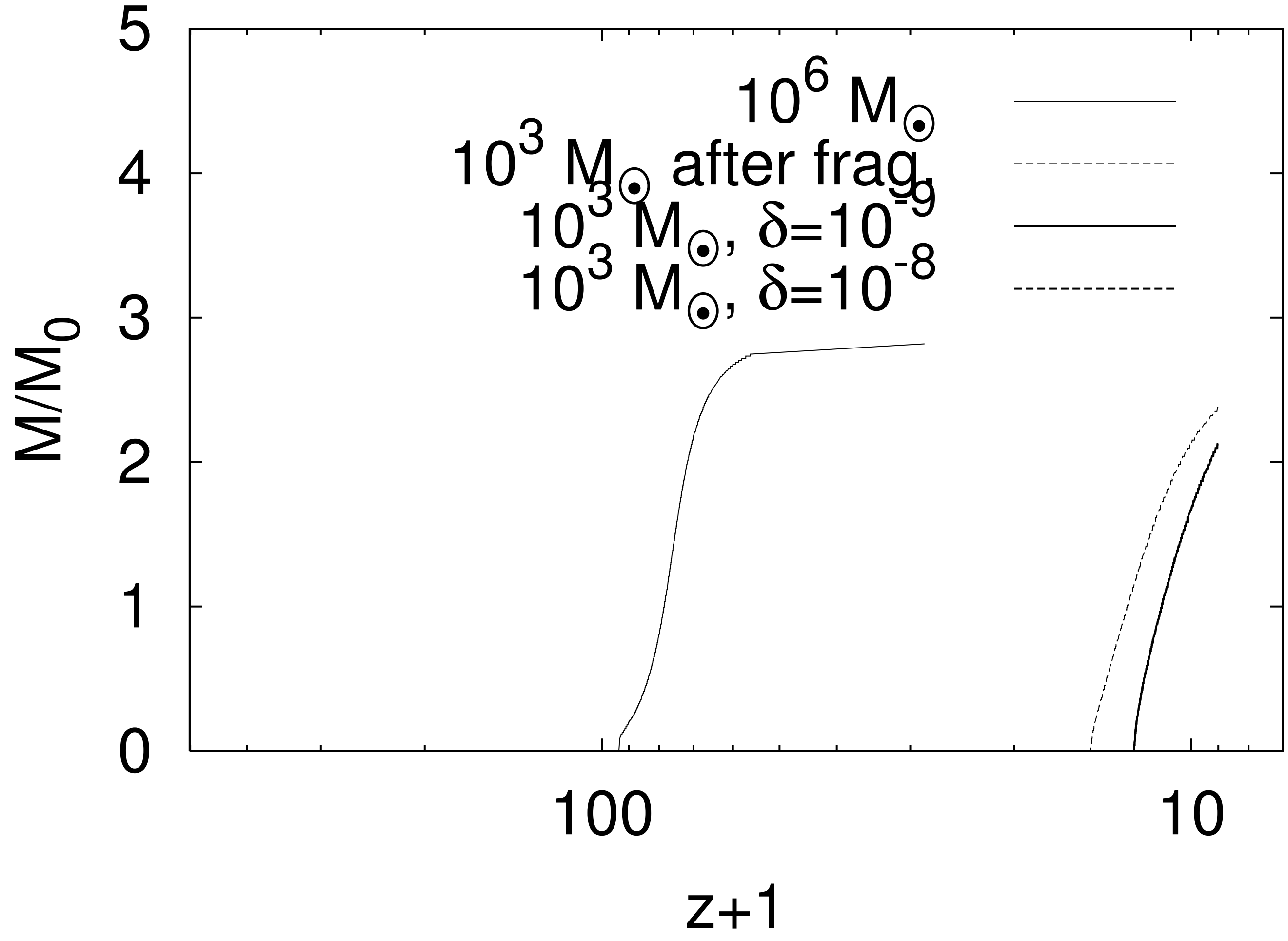

Fraction of collapsed mass for the 'standard' $\boldsymbol{a_0}$: $\mathbf{10^6} \boldsymbol{M_\odot}$ $\mathbf{10^{-9}}$, $\mathbf{10^3} \boldsymbol{M_\odot}$ after fragmentation, $\mathbf{10^3} \boldsymbol{M_\odot}$ $\mathbf{10^{-9}}$ and $\mathbf{10^3} \boldsymbol{M_\odot}$ $\mathbf{10^{-8}}$.

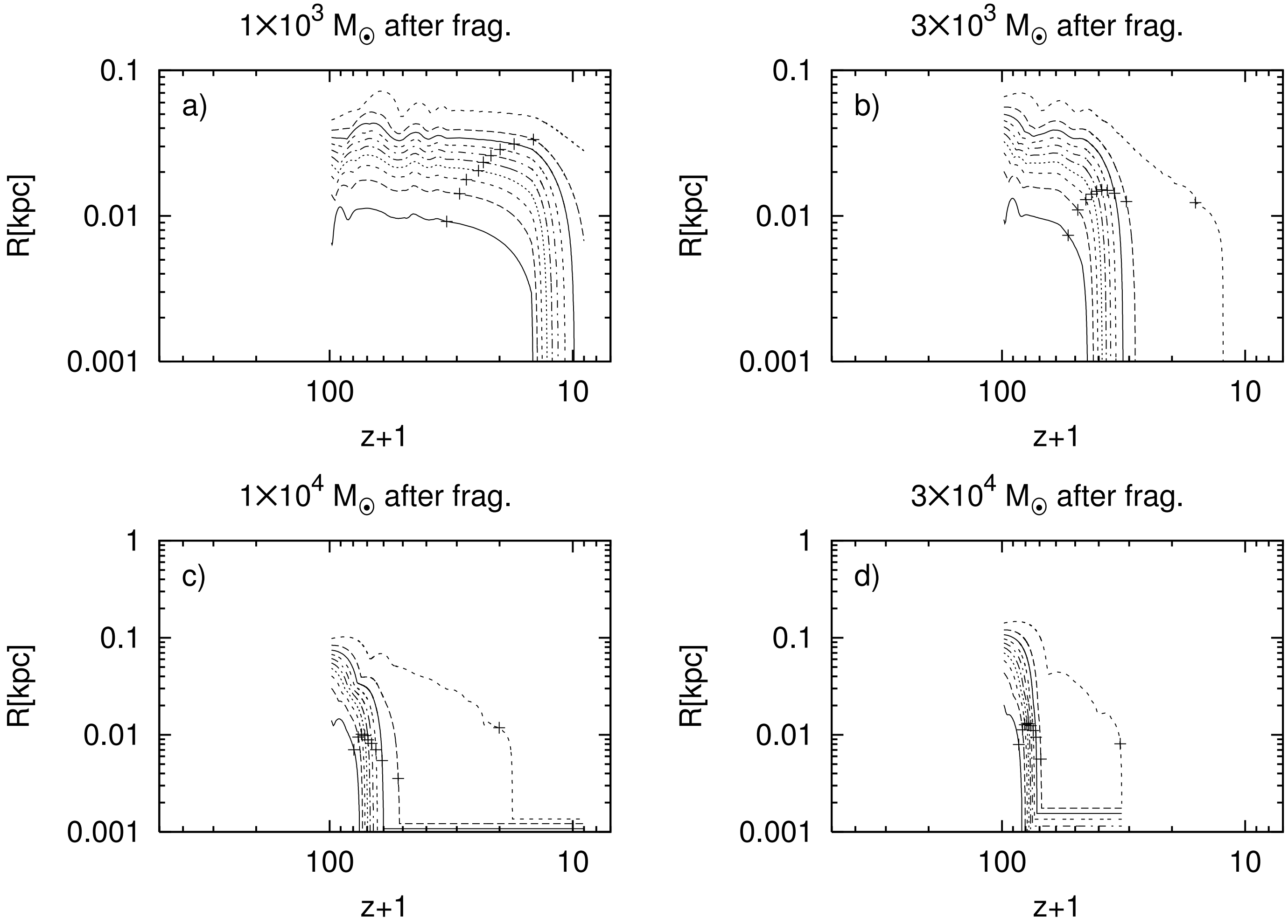

Shell trajectories for clouds with masses equal to $\mathbf{1} \times \mathbf{10}^3 M_\odot$, $\mathbf{3} \times \mathbf{10}^3 M_\odot$, $\mathbf{1} \times \mathbf{10}^4 M_\odot$ and $\mathbf{3} \times \mathbf{10}^4 M_\odot$ after fragmentation.

We can see that apart from some oscillations at the beginning, evolution of a re-scaled cloud is very similar to the evolution of single clouds of the same mass. Simply its mass is so low that it cannot cool efficiently and it finally collapses at nearly the same redshift as clouds that were collapsing directly.

The $10^6 M_\odot$ cloud collapses very fast, about $z \sim 80$. The final slow-down is caused by the fact that for the last shell corresponding to the bound mass M_z mean density contrast inside is zero and it expands due to the Hubble flow. Collapse for $10^3 M_\odot$ clouds with 10^{-9} and 10^{-8} initial overdensities is almost indistinguishible and it starts about $z + 1 = 12.5$ while for the re-scaled cloud it is somewhat faster and it starts about $z + 1 = 14.6$.

If we compare the evolution of re-scaled clouds with various masses, we note some similarities: oscillations at the beginning and final collapse a bit earlier than for single clouds of the same mass. However, with increasing mass oscillations are less and less important. For $\mathbf{3 \times 10}^4 \boldsymbol{M}_\odot$ the collapse is too fast for oscillations to affect significantly further evolution.

5. Conclusions.

Wilkinson MAP results suggest that reionization occured about $z \sim 20$. It means that the first bound objects should have been formed even earlier, perhaps about $z \sim 30$. Our previous simulations (Stachniewicz, Kutschera 2003) show that if we assume ΛCDM models and take recent estimates of Ω_M and Ω_Λ, direct formation of low-mass objects that could possibly reionize the Universe before $z \sim 10$ is very unlikely. Moreover, our fragmentation-related calculations make us doubt if including possible fragmentation of greater clouds could speed up the collapse enough – even if some low mass cloud has greater overdensity than directly forming ones, it still needs some time to cool down.

In contrast, MOND seems to provide a good way to solve that problem. For the 'standard'$\boldsymbol{a}_0$ clouds of mass $\boldsymbol{3 \times 10^3 M_\odot}$ or heavier may collapse about $\boldsymbol{z \sim 30}$ so they or their cores may form the first stars and quasars. For lower $\boldsymbol{a}_0$ only objects of mass $\boldsymbol{3 \times 10^4 M_\odot}$ or greater may be formed directly before $\boldsymbol{z \sim 30}$. We think it favours the 'standard' value but, however, one would need to perform full 3-D simulations to give more definite answer.

6. Summary.

If our assumptions about MOND were correct, its predictions seem to be more consistent with early reionization suggested by WMAP results (Bennett et al., 2003 etc.) than the ones of the most recent ΛCDM models. This does not prove that MOND is correct and ΛCDM not but, however, it suggests that perhaps cosmologists should pay more attention to MOND because it seems to be an interesting alternative to models with non-baryonic dark matter.

Bibliography.

Bennett C. L. et al., 2003, astro-ph/0302207

Haiman Z., Thoul A. A., Loeb A., 1996, ApJ 464, 523

Milgrom M., 1983, ApJ, 270, 371

Milgrom M., 2002, New Astronomy Reviews, 46, 741

Sanders R. H., 1998, MNRAS, 296, 1009

Sanders R. H., Verheijen M. A. W., 1998, ApJ, 503, 97

Seljak U., Zaldarriaga M., 1996, ApJ 469, 437

Stachniewicz S., Kutschera M., 2001, APPolB 32, 227

Stachniewicz S., Kutschera M., 2001, APPolB, 32, 3629

Stachniewicz S., Kutschera M., 2003, MNRAS, 339, 616

Thoul A. A., Weinberg D. H., 1995, ApJ, 442, 480